New aeroelastic studies for a morphing wing

Samuel COURCHESNE[1], Andrei Vladimir POPOV[1], Ruxandra Mihaela BOTEZ*,[1]

*Corresponding author
*,[1] École de technologie supérieure, Montréal, Québec, H3C 1K3, Canada
Ruxandra.Botez@etsmtl.ca

DOI: 10.13111/2066-8201.2012.4.2.2

Abstract: *For this study, the upper surface of a rectangular finite aspect ratio wing, with a laminar airfoil cross-section, was made of a carbon-Kevlar composite material flexible skin. This flexible skin was morphed by use of Shape Memory Alloy actuators for 35 test cases characterized by combinations of Mach numbers, Reynolds numbers and angles of attack. The Mach numbers varied from 0.2 to 0.3 and the angles of attack ranged between -1° and 2°. The optimized airfoils were determined by use of the CFD XFoil code. The purpose of this aeroelastic study was to determine the flutter conditions to be avoided during wind tunnel tests. These studies show that aeroelastic instabilities for the morphing configurations considered appeared at Mach number 0.55, which was higher than the wind tunnel Mach number limit speed of 0.3. The wind tunnel tests could thus be performed safely in the 6'×9' wind tunnel at the Institute for Aerospace Research at the National Research Council Canada (IAR/NRC), where the new aeroelastic studies, applied on morphing wings, were validated.*

Key Words: *morphing configurations, laminar airfoil, XFoil code, aeroelastic studies, flutter conditions, wind tunnel tests*

I. INTRODUCTION

Research into drag reduction, which often leads to fuel consumption reduction, was launched by the aerospace industry over the last few years, due to worldwide environmental concerns and rising fuel costs. Drag reduction can be achieved by airfoil shape modification, with the aim of delaying the flow transition from laminar to turbulent, by moving the transition point close to the wing trailing edge. The laminar flow past an aerodynamically morphing wing can be improved so as to obtain significant drag reduction. This concept of modifying the airfoil for various flight conditions is known as a 'morphing wing'.

Various morphing wing studies have been conducted. One consists of a symmetric wing structure with two tapered graphite/epoxy composite plates and a steel body. Four pairs of SMA wires are attached to the wings' bottom surfaces in a chord-wise direction. Lift and drag forces are measured at various angles of attack. Dynamic vibration signals, measured by fiber Bragg grating (FBG) sensors at the wing root, are used to monitor aeroelastic unstable phenomena, such as flutter at various angles of attack [1].

Another wing structure, comprised of an optimized internal layout of cables and struts, was able to morph itself. Cables were used as actuators while struts provided rigidity to the wing. In addition to achieving continuous morphing by changing cable lengths, this structure had the advantages of being lightweight and having a distributed actuation.

The Non-dominated Sorting Genetic Algorithm II (NSGA II) was used for the NASA HECS and the NextGen TSCh wing modeling [2]. Improved wing roll performance was achieved by use of articulated conformal control surfaces. The analysis results were compared to the experimental results obtained for a 16% scale model of a fighter wing

equipped with embedded smart materials used to deform a control surface. The control surface design was found suitable for low-rate applications such as take-off and landing configurations [3].

The present work refers to a morphing wing equipped with Shape Memory Alloys which modify the wing's upper surface morphing flexible skin for various test cases – and for which the transition point moves close to the wing airfoil trailing edge.

This rectangular wing model incorporated two parts:

- A fixed rigid part of the wing's lower surface, which sustains all of the resistance forces, and
- The upper wing surface, consisting of a flexible skin which changes its shape through electrically controlled shape memory alloy actuators (see Figure 1).

Aerodynamic changes in the boundary layer flow took place over the morphing upper wing surface – therefore the transition point position changed and moved closer to the wing airfoil's trailing edge.

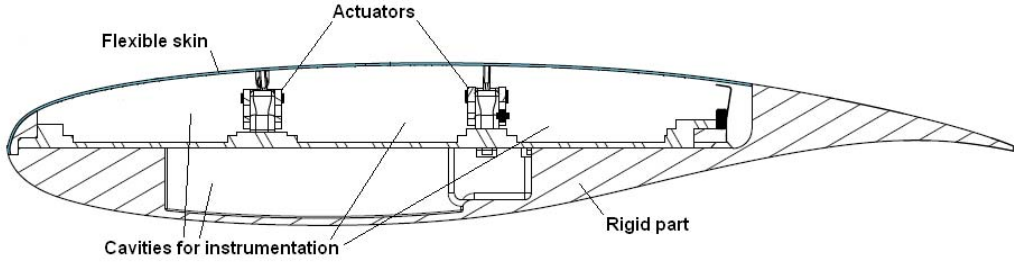

Fig. 1 Cross-section of the morphing wing model

The wing's lower surface was designed and manufactured by a team from the Institute of Aerospace Research – Canada National Research Council, while the morphing upper wing surface and the Shape Memory Alloy (SMA) actuators were designed and manufactured by the Memory Alloys and Intelligent Systems Laboratory (*Laboratoire sur les alliages à mémoire et sur les systèmes intelligents*) LAMSI team at ETS [4].

A laminar airfoil was considered as a reference airfoil shape for the morphing wing studied here, since a series of optimized airfoils had already been designed and calculated by the Ecole Polytechnique team using XFoil CFD code for various airflow conditions expressed as combinations of angles of attack and Mach numbers [5]).

Each optimized airfoil shape was characterized by its closest transition point location to the trailing edge.

In total, 35 optimized airfoils were designed for the airflow combinations of Mach numbers 0.2, 0.225, 0.25, 0.275, 0.3 and angles of attack -1, -0.5, 0, 0.5, 1, 1.5 and 2 deg.

Aeroelastic analyses were performed on the flexible skin of the morphing wing for all 35 flight cases, prior to its testing in the wind tunnel, in order to determine if the wing would be stable in terms of flutter (i.e., no flutter would occur), and so the wing would therefore not be mechanically destroyed during its testing in the wind tunnel. Finite Element methods, coupled with KE methods, were used for structural and flutter analyses with the Nastran/Patran commercial software.

The wind tunnel tests were performed at the Institute for Aerospace Research at the National Research Council Canada in the 6 ft x 9 ft Subsonic Wind Tunnel.

The purpose of these tests was to assess the performance of the wing model with a morphing skin with the goal of improving the laminar flow over the upper wing surface. The

upper wing surface, made of flexible skin, was controlled and morphed by smart material actuators at two control points, such that any optimized upper airfoil shape for the 35 flow conditions could be achieved by adjusting the vertical displacements of both actuators. Different techniques of control were used in this project in order to verify and validate the open and closed loop. For the validation of the laminar flow controller, real time optimization [6], *On-Off and Proportional-Integral* PI ([7], [8]), bi-positional and PI laws optimimum combination [9] techniques, as well as other modern techniques such as fuzzy logic [10] were used.

The flutter analysis showed that flutter occurred at a Mach number equal to 0.55, and thus, since that is higher than the upper limit wind tunnel Mach number of 0.3, the wind tunnel tests could safely take place.

II. AEROELASTIC ANALYSIS

The commercial software for finite element analysis, MSC/NASTRAN, was used to build the 3D numerical model of the flexible skin upper surface which was situated between 3% and 70% of the wing chord, as shown in Figure 2.

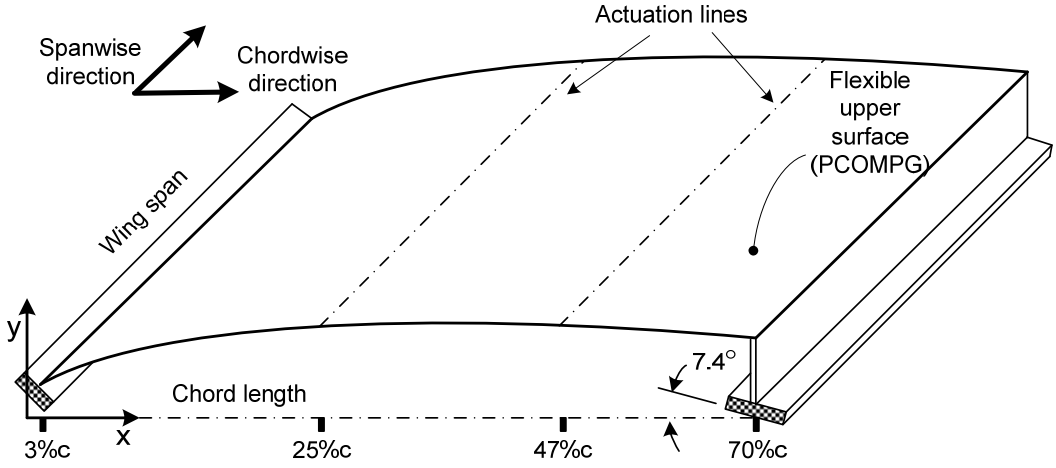

Fig. 2 Flexible extrados schematic with boundary and loading conditions

A. Finite element modeling

The structural model was defined using the GRID and CQUAD4 shell elements given by the MSC/NASTRAN commands [11].

The structure was divided into several bands of equal widths along the span, and formed elements in the chord-wise defining the airfoil shape; the whole formed a structure of 406 plane elements as shown in Figure 3 (a).

The internal elements were composed of four layers of composite materials. The MAT8 command defined the Young's modulus, the shear modulus, the Poisson's ratio and the density.

All of the leading edge nodes were constrained to simulate a perfect clamp. In addition, the trailing edge was also well constrained, with the exception of the translation motion in its chord-wise aspect.

To simulate the compensation spring, all the nodes along the actuators axis were constrained in translation and free in rotation, thus simulating the mechanism. Finally, all of

the nodes were constrained against plane rotation, as the CQUAD4 element had no rigidity in this condition.

The ASET1 command was considered to reduce the problem size in order to restrict the number of freedom degrees for the wing normal deflection, i.e. the translation along the Z axis (the degree of freedom that allows wing bending and torsion), which is the only deflection required for aerodynamic force determination.

It is important to note that the plan or shell model is often used because it provides results as close to reality as possible without overly complicating the problem.

The material density, configured by entering the MAT8 command and the parameter COUPMASS, 1, resulted from generation of the coupled plate elements mass matrices, while the GRAV command introduced the model weight in the problem. Although the model weight in the wind tunnel was relatively low, it was not neglected, and the angles of attack remained small.

B. Aerodynamic modeling

The AERO command was used for the aerodynamic modeling, in which the basic coordinate system was used as the aerodynamic coordinate system.

Physical parameters were defined, such as the sea level density and the reference chord length equal to 334.8 mm. The commands SYMXZ = 1 for a complete wall reflection of the wind tunnel and SYMXY = 0 were defined, neglecting the floor tunnel or ceiling interference. The CAERO1 command, including a subsonic Mach number in the TRIM command, specified the use of the aerodynamic Doublet-Lattice Panel theory. A minimum of six equal strip widths along the span-wise was specified, along with a minimum of four equal strip widths along the chord-wise section.

The aerodynamic and the structural models were interconnected with a spline surface, SPLINE1. The 24 aerodynamic boxes correspond to 232 nodes listed by the SET 1 command. The 232 nodes were variously spaced along the span-wise section from one extremity to another. The PAERO1 command was required even if no interference problem occurred. The model division in aerodynamic boxes is shown in Figure 3(b).

The MKAERO1 command provided the required data for the aerodynamic matrix interpolation into the flutter solution. For each Mach number tested, the reduced frequencies $k = 0.001$ to $k = 0.90$ were specified to determine the flutter speed.

The Lagrange method was used for the vibration analysis in the EIG|R command to obtain the ten modes that had the largest normalized assembly components. Each optimized airfoil shape was obtained by use of the XFoil CFD code.

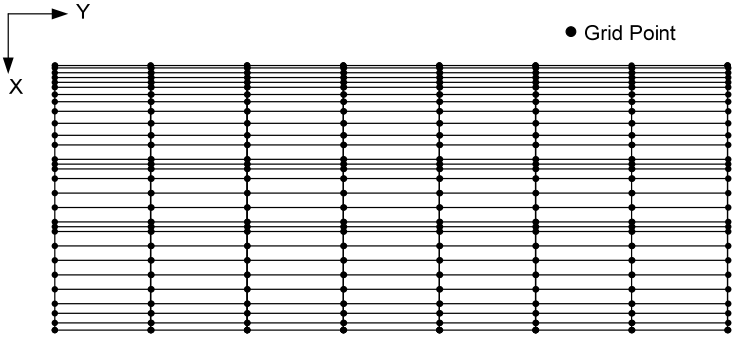

(a) Structural model

1XX Element Aero Box

101	105	109	113	117	121
102	106	110	114	118	122
103	107	111	115	119	123
104	108	112	116	120	124

(b) Aerodynamic model

Fig. 3 Structural and aerodynamic model

C. Flutter analysis method

The KE flutter analysis method was chosen for the system dynamics determination. This flutter method was chosen based on its efficiency at producing well-behaved *V-g* curves.

The structural damping was introduced by the parameter PARAM, KDAMP, -1 and the table TABDMP1.

Since no damping data was known, we assumed $g = 0.01$ at a frequency of 1000 Hz. The FLUTTER command specified the use of the KE flutter analysis method.

The FLFACT command gives information during wind tunnel tests on the density ratio, the Mach number, and the reduced frequencies set, and specifies a linear interpolation of generalized aerodynamic force coefficients.

The flutter speeds were converted from mm/s into m/s using the instruction PARAM, VREF, 1000.0.

III. RESULTS AND DISCUSSION

The mass and inertial data, the vibration frequencies and the deflection modes for the analyzed nodes (ASET1) were calculated.

The Lagrange method was used for vibration analysis, using the command EIGR to obtain ten modes which have frequencies up to 100 Hz.

A. Model's dynamic response (Modal Analysis)

In the modal analysis method, prior to the flutter analysis, two solving techniques were available to determine a response to an imposed displacement.

The first method is the large mass method, and the second is the Lagrangian multiplier method.

The Lagrangian multiplier method required less computation and was very efficient for a small number of modes (in our case, the parameter PARAM, LMODES, 10 specified that the ten first modes of vibration be included in the flutter problem formulation for a frequency spectrum covering 100 Hz); this method was widely used for its efficiency in several aeroelastic dynamic response analyses and the results are presented in Table I.

Table I Dynamic results of the flexible extrados

Mode Sorted	Mode Remarks	Freq (Hz)
MODE-1	1st Symmetric rotation (6 waves) between Act. #2 and T.E.	9,542
MODE-2	1st Asymmetric rotation (6 waves) between Act. #2 and T.E.	9,818

MODE-3	2nd Asymmetric rotation (6 waves) between Act. #2 and T.E.	26,198
MODE-4	2nd Asymmetric rotation (5 waves) between Act. #2 and T.E.	41,180
MODE-5	3th Asymmetric rotation (4 waves) between Act. #2 and T.E.	57,236
MODE-6	3th Symmetric rotation (3 waves) between Act. #2 and T.E.	58,037
MODE-7	4th Asymmetric rotation (2 waves) between Act. #2 and T.E.	58,872
MODE-8	1st Symmetric bending (2 waves) between Act. #2 and T.E.	75,462
MODE-9	1st Asymmetric rotation (8 waves) between Act. #1 and Act. #2	93,809
MODE-10	1st Symmetric rotation (7 waves) between Act. #1 et Act. #2	100,980

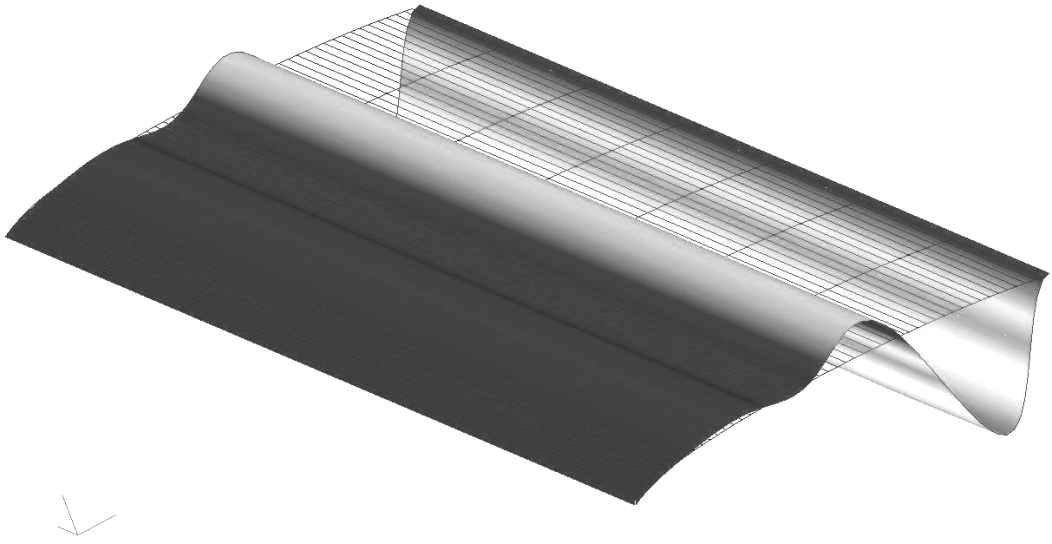

Fig. 4 First symmetric bending mode located between actuator #1 and the trailing edge (75,462 Hz)

B. Flutter analysis numerical results

The structural stiffness, mass and damping matrices for the aeroelastic flutter analysis were generated by use of MSC.Nastran by following an analysis of aeroelastic flutter. The aerodynamic operator matrix was generated from data describing the aerodynamic finite elements' geometry.

The aerodynamic model choice of "grid points" was independent of the structural "grid points" positions called "nodes".

The subsonic flow theory is the Doublets-method that allows coupling of the aerodynamical elements to the structural body.

Thus, the vibration modes of the structure were used in the dynamic analysis and the following equation is used to determine the model characteristics, following the flutter analysis algorithm (SOL 145) proposed by the Nastran software.

$$\left[M_{hh}\, p^2 + \left(B_{hh} - \rho c V Q^I_{hh} \Big/ 4k \right) p + \left(K_{hh} - \rho c V^2 Q^R_{hh} \Big/ 2 \right) \right] \{ u_h \} = 0$$

This equation assumes a simple harmonic motion $\{u(t)\} = \{u_h\}e^{i\omega t}$, presented in the form of a second order differential equation describing the dynamic linear behavior of the structure which is subject to forces and moments caused by the fluid flow. Figure 5 shows a flowchart that describes the software steps for this calculation.

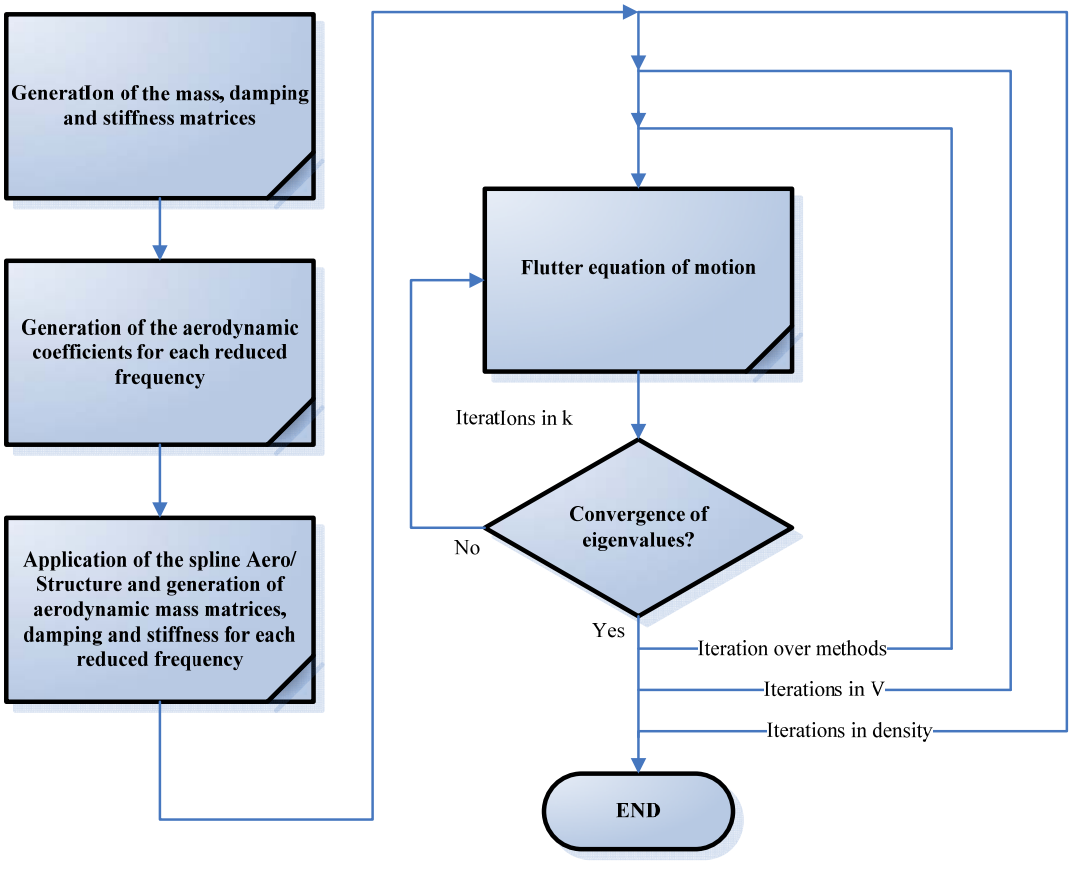

Fig. 5 Flowchart of the flutter solution to the equation of motion (for one Mach number)

The *V-g* flutter analysis method was used. In this method, the structural damping, *g*, of all of the vibration modes was assumed to be an unknown value.

In Figure 6, all of the mode shapes are shown, except for modes 5, 7 and 9, which correspond to under-damped modes.

The first ten modes were analyzed and graphically presented in the forms of frequencies and damping versus speeds.

It is known that the flutter speed is the speed at which the damping is zero (see the first curve showing the damping variation with speed).

Then, the corresponding model's flutter frequencies were calculated from the second graph which shows the frequency variation with speeds.

The advantage of the numerical approach is that only aerodynamic forces need to be determined for real frequencies.

The disadvantage is that it is not possible to have a physical response overview. For a system with damping, only at the speed $V = V_F$ (i.e. where $\omega = \omega_R$ and $\omega_I = 0$) will the mathematical solution provides the physics of this problem.

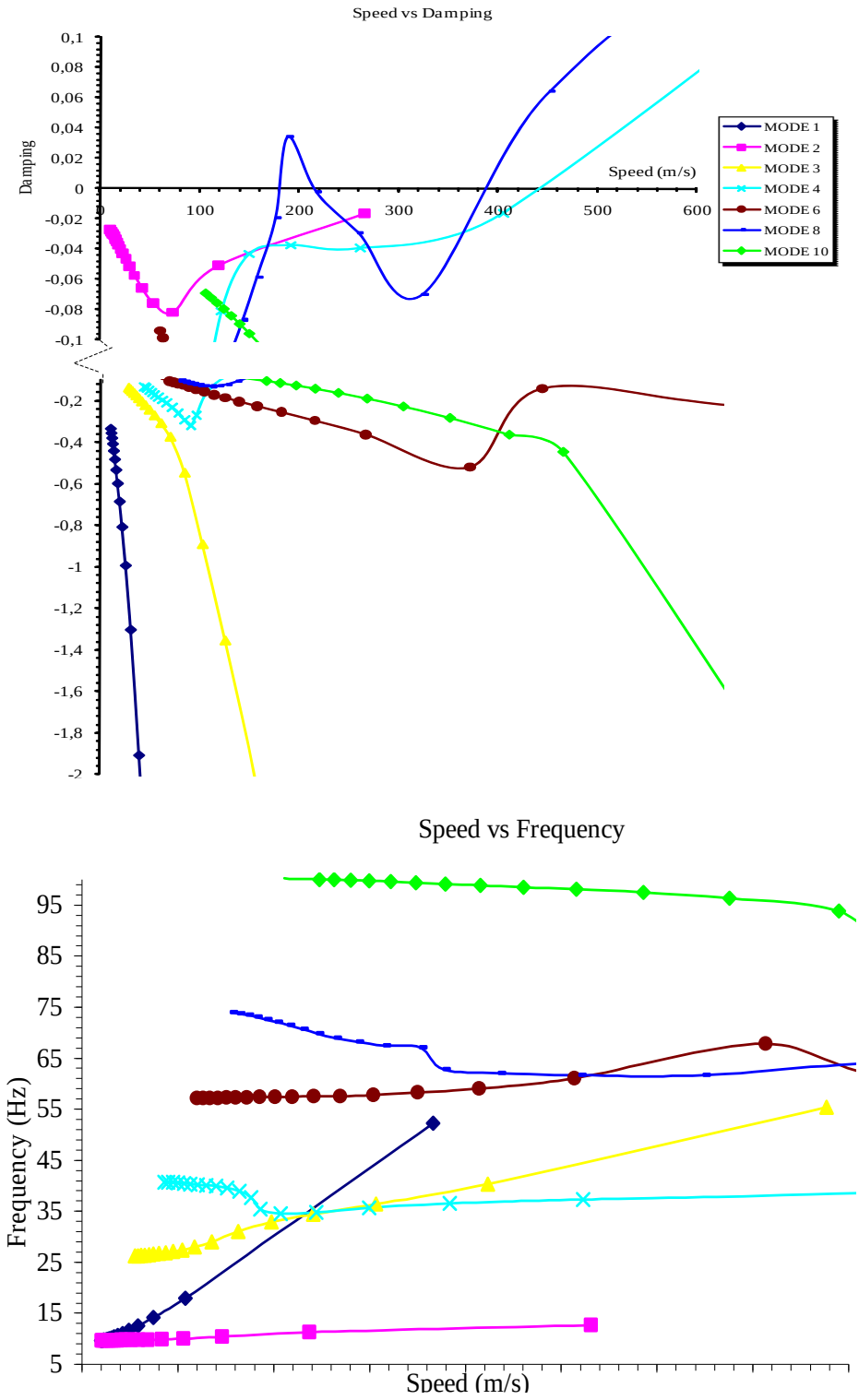

Fig. 6 Damping and frequency versus speeds

Following a flutter analysis, the wing or aircraft design can be modified to prevent flutter, prior to its manufacturing or wind tunnel or in-flight testing. The key design parameter is the maximum flight speed V_d.

The ratio between the absorbed energy and the dissipated energy depends on the flow speed. A stable oscillation could occur when this ratio is harmonic.

The flow speed is critical when the oscillations become unstable. A model can have a variety of flutter modes.

Ideally, the lowest critical speed exceeds the highest possible flight speed by a reasonable safety margin.

The critical flutter speeds for each configuration and their corresponding frequencies are shown in Table II.

The safety factor offered by the FAR 25 [12] standard specifies that the critical flutter speed is 1.2 times the flight design speed (V_d), which varies from 68m/s to 102 m/s depending on flight conditions. The (V_P/V_d - 1) * 100 value gives the model's percentage margin and this value should be greater than 20%. The differences between flight configuration results are shown in Table II.

Table II Flutter results of the model

Flight speed (Mach number)	Flight speed (V_d) in m/s	Flutter speed (V_F) in m/s	Flutter frequencies (Hz)	Differences (%)
0.2	68	186.122	67.2403	173.71
0.225	76.5	186.130	67.2434	143.31
0.25	85	186.141	67.2472	118.99
0.275	93.5	186.153	67.2516	99.09
0.3	102	186.167	67.2567	82.52

The flutter phenomenon only occurred for the Mach number of 0.55. For the flight configurations studied, the flutter margin was found to be 20% above the flight speed and thus met the FAR 25 standard.

During wind tunnel tests for different configurations at the maximum Mach number of 0.3, no flutter problem occurred, thus demonstrating the efficiency of the wing aeroelastic analysis.

IV. CONCLUSION

During flight, the inertial loads (gravity, centrifugal force, gyroscopic) and the elastic loads arising from structure deformations must be considered. The mutual interactions between these loads: aerodynamic, inertial and elastic, were evaluated for aeroelastic adaptive wing studies.

Following the analysis of the flexible wing upper skin surface by use of Nastran software, it was possible to demonstrate that the flutter phenomenon did not occur for the flight conditions tested in the wind tunnel.

It was clear that the numerical predictions reflected the wind tunnel tests results, as no damage from flutter occurred during these tests. The aeroelastic studies on a morphing wing presented in this paper are original.

In the development of further work, it would be interesting to conduct a flutter analysis by dynamically changing the airfoil shape (over several iterations), since flutter is influenced so much by a model's geometry.

In addition, a better approximation of the stiffness constants from the actuators' rows would lead to the calculation of more accurate frequencies.

Aeroservoelasticity studies could also be performed by studying the interactions between the aeroelastic model and the optimized controller using fuzzy logic algorithms. The controller algorithms have already been tested and successfully validated in a wind tunnel.

Acknowledgments

We would like to thank CRIAQ (Consortium of Research in the Aerospatial Industry in Quebec), Thales Avionics, Bombardier Aerospace, NSERC (National Sciences and Engineering Research Council) and NRC (National Research Council) for providing the funding for this research. In particular, we want to thank Mr. George Henri Simon for initiating the CRIAQ 7.1 project as well as Mr. Philippe Molaret from Thales Avionics and Mr. Eric Laurendeau from Bombardier Aerospace for their collaboration on this work.

REFERENCES

[1] R. Barrett, *Improvements to commercial and general aviation via adaptive aerostructures*, *Paper AIAA-2007-7873*, 7th AIAA Aviation Technology, Integration and Operations Conference (ATIO), 18-20 September, pp. 1-9. 2007[2] S. Bharti, et al., *Optimal structural design of a morphing aircraft wing using parallel nondominated sorting genetic algorithm* II (*NSGA* II), Smart Structures and Materials 2006: Industrial and commercial applications of smart structures technologies, edited by D. K. Lindner, Proceedings of SPIE Vol. **6166**, pp. 1-12, 2006.

[3] B. Sanders, et al., Aerodynamic and aeroelastic characteristics of wings with conformal control surfaces for morphing aircraft, *Journal of Aircraft*, Vol. **40**(1), pp. 94-99, ISSN (printed): 0021-8669. ISSN (electronic): 1533-3868, 2003**.**

[4] D. Coutu, V. Brailovski, P. Terriault, Promising Benefits of an Active-Extrados Morphing Laminar Wing, *Journal of Aircraft*, Vol. **46**(2), pp. 730-731, ISSN (printed): 0021-8669. ISSN (electronic): 1533-3868, 2009.

[5] L. Pagès, O. Trifu, I. Paraschivoiu, Optimized Laminar Flow Control on an Airfoil using the Adaptable Wall Technique, *Proceedings of the CASI Aero 2007 Symposium*, June 2007.

[56] A.-V. Popov, R. M. Botez, L. T. Grigorie, M. Mamou, Y. Mebarki, Real time airfoil optimization of a morphing wing in wind tunnel, *AIAA Journal of Aircraft*, Vol. **47**(4), pp. 1346-1354, 2010.

[7] L. T. Grigorie, A.-V., Popov, R. M. Botez, M. Mamou, Y. Mebarki, On-Off and Proportional-Integral Controller for a Morphing Wing. Part 1: actuation mechanism and control design, *Proceedings of the Institution of Mechanical Engineers*, Vol. **226**(2), Part G, *Journal of Aerospace Engineering*, pp. 131-145, 2012.

[8] L. T. Grigorie, A.-V., Popov, R. M. Botez, M. Mamou, Y. Mebarki, On-Off and Proportional-Integral Controller for a Morphing Wing. Part 2: control validation - numerical simulations and experimental tests, *Proceedings of the Institution of Mechanical Engineers*, Vol. **226**(2), Part G, *Journal of Aerospace Engineering*, pp. 146-162, 2012.

[9] L. T. Grigorie, R. M. Botez, A.-V., Popov, Morphing wing used shape memory alloy actuators new control technique with bi-Positional and PI laws optimum combination – Numerical and experimental validation, *Lecture Notes in Electrical Engineering*, Springer-Verlag Edition, 2011.

[10] L. T. Grigorie, R. M. Botez, A.-V., Popov, 2012, Fuzzy logic control of a smart actuation system in a morphing wing, *Fuzzy Controllers*, ISBN: 979-953-307-843-3, INTECH Edition, 2012.

[11] MSC/Nastran documentation (MSC software corporation, USA), 2001.

[12] FAR 25 Aviation Regulations, 2000.